Hindawi
Journal of Mathematics
Volume 2022, Article ID 1476607, 9 pages
https://doi.org/10.1155/2022/1476607

Research Article

Sensitivity and Optimal Control Analysis of an Extended SEIR COVID-19 Mathematical Model

C. M. Wachira,[1] **G. O. Lawi**,[1] **and L. O. Omondi**[2]

[1]*Department of Mathematics, Masinde Muliro University of Science and Technology, Kakamega, Kenya*
[2]*Department of Mathematics, Egerton University, Njoro, Kenya*

Correspondence should be addressed to C. M. Wachira; cwachira@mmust.ac.ke

Received 24 August 2022; Revised 23 September 2022; Accepted 7 October 2022; Published 15 October 2022

Academic Editor: Kenan Yildirim

In this paper, a mathematical model based on a system of ordinary differential equations is developed with vaccination as an intervention for the transmission dynamics of coronavirus 2019 (COVID-19). The model solutions are shown to be well posed. The vaccine reproduction number is computed by using the next-generation matrix approach. The sensitivity analysis carried out on this model showed that the vaccination rate and vaccine efficacy are among the most sensitive parameters of the vaccine reproduction number, R_V. The optimal control problem is solved with the rate of vaccination and the transition rate from the vaccinated class to the infected class as control variables. Finally, the numerical simulations showed that the control intervention should aim to increase the vaccination rate with a high-efficacy vaccine.

1. Introduction

COVID-19 is a highly contagious respiratory disease caused by the novel severe acute respiratory syndrome coronavirus–2 (SARS-CoV-2). The increasing prevalence rate of the virus nearly devastated healthcare systems across the world [1, 2]. On March 11, 2020, the World Health Organization (WHO) declared the disease a global health pandemic. It is transmitted through inhalation of respiratory droplets from an infectious person emitted through sneezing, coughing, and having a close conversation, as well as contact with contaminated surfaces [3]. The infection prominently affects the respiratory tract. The initial COVID-19 symptoms are fever, dry cough, and fatigue. Other symptoms include body aches and pains, a sore throat, diarrhoea, headache, loss of taste and smell, breathing difficulties, skin rash, and discoloration of the fingers and toes [3].

COVID-19 morbidity and mortality can be compounded by pre-existing diseases such as cardiovascular disease, respiratory disease, cancer, infectious diseases, and substance abuse. Furthermore, pre-existing conditions such as environmental, demographic, and socioeconomic factors may influence the COVID-19 incidence rate [4]. To prevent and control the spread of COVID-19, health providers and governments around the world implemented containment measures such as lockdowns, travel bans, cessation of movement, social distancing, proper hygiene, and proper hand washing, among others. Despite these safeguards, the virus continues to spread, although at a slow rate.

Vaccination has been a major public health tool in modern medicine used to minimize the impact of many infectious diseases on humans [5, 6]. A vaccine is any biologically derived substance that elicits a protective immune response when administered to a susceptible host. Vaccines help the body to prepare for disease by taking the advantage of the fact that immunity knows how to defend against infectious organisms, which are typically viruses, bacteria, or toxins [7]. Given the emergence of highly transmissible new variants, decreased vaccine effectiveness, and unequal vaccine availability, there is a growing concern that vaccination may not result in herd immunity. Vaccines reduce the risk of severe disease and death; therefore, a country's vaccine coverage must be high in order to protect the healthcare system from an infection surge [2]. Since late 2020, several SARS-CoV-2 variants of concern that are more transmissible and/or vaccine-resistant have been identified [8].

In modern medicine, vaccination has been an important public health technique for reducing the burden of many human infectious diseases [5, 6, 9]. Several COVID-19 vaccine candidates have been developed and are already in use [10]. Vaccines such as Pfizer, Moderna, AstraZeneca, Sputnik, Sinopharm, Johnson & Johnson, and many others are currently being administered around the world to date. It is a social responsibility choice of an individual to get vaccinated. However, offsetting the fear and adverse side effects of the vaccine has to be carried out[11]. The shortage of supply of COVID-19 vaccines in many developing countries has resulted in the implementation of different immunization strategies, with varying results. For example, in Kenya, prioritization is given to the adult population [2].

A mathematical model provides insight into infectious disease transmission and control [12, 13]. Many mathematical models on the dynamics of COVID-19 with control strategies have been developed and studied, for example, in studies carried out in [9, 10]. Optimal control is regarded as a powerful mathematical tool for optimizing control problems in various fields [14–18]. In the context of vaccination, the dynamics of disease transmission and immunity in a population are typically modelled by using network compartmental approaches [19]. A mathematical model for the dynamics of COVID-19 is presented in [18]. An optimal control function is added to the model in order to effectively control the outbreak. The main controls are isolation, quarantine, and hospitalization. The result shows that adopting the available control measures to their full potential will greatly reduce infectious populations.

A new COVID-19 model with an optimal control analysis is presented in [20]. The authors considered four different controls to develop an optimal control model, including prevention, vaccination control, rapid screening of people who are exposed, and people who are infected without screening. The forward-backward Runge–Kutta method is used to resolve the model with and without control. The findings suggest that control can be useful for reducing infected individuals and improving population health. A novel fractional-order mathematical model that explains the behaviour of COVID-19 in Ethiopia is developed and analyzed in [21]. An inexact Newton iterative method is used to solve the model system. The model considers the impact of various control techniques on disease transmission.

Zamir et al. in [22] developed a mathematical model to study the transmission dynamics of COVID-19. The study used a nonclinical approach to investigate optimal control. A COVID-19 mathematical model that takes into account the susceptible, exposed, infected, asymptotic, quarantine/isolation, and recovered classes is developed and analyzed in [23]. Elasticity and sensitivity analysis shows that the model is more sensitive to transmission rates from infected to exposed classes than transmission rates from susceptible to exposed classes.

Alqarni et al. [24] developed a new mathematical model for the transmission dynamics of the coronavirus (COVID-19) using cases reported in the Kingdom of Saudi Arabia from March 2, 2020, to July 31, 2020. The model's stability results are shown when the basic reproduction number is $R_0 < 1$, and the model is locally asymptotically stable. Using the PRCC method, they show some important parameters that are more sensitive to the basic reproduction number R_0. The sensitive parameters that act as control parameters and can reduce and control infection in the population are depicted graphically. The study results suggested that if controls are followed, the infection rate in the Kingdom of Saudi Arabia can be reduced significantly. In this study, an extended SEIR COVID-19 dynamics model with vaccination is proposed to investigate the impact of vaccination as a control intervention on the pandemic spread.

2. Model Formulation

A susceptible-vaccinated-exposed-infected-recovered (SVEIR) model with a standard incidence rate is developed and analyzed. Despite the fact that there are underlying conditions that predispose someone to a higher risk of contracting COVID-19 disease, the population under study is assumed to have an equal level of susceptibility. Individuals in this category are known as susceptible individuals denoted by $S(t)$. Several COVID-19 vaccine candidates have been developed and are already in use [10]. Individuals who have been vaccinated are hereby categorised as the vaccinated class, denoted by $V(t)$. When susceptible individuals are exposed to the virus, they undergo an incubation period, which is the time between virus exposure and the onset of symptoms. This is on average 5–6 days, but it can be as long as 14 days [25]. The incubating individuals in this study are categorised as the exposed class denoted by $E(t)$. Following the end of the exposure period, the incubating individual's transit into the infection class is denoted by $I(t)$. The infectious potential of COVID-19 is significantly greater just before or within the first five days of symptom onset [26]. The infected class $I(t)$, in this study, includes both presymptomatic and asymptomatic cases. Depending on the severity of symptoms and the intervention strategies in place, the infected individuals may die or recover from the disease. Thus, the class $R(t)$ denotes the number of individuals who have recovered from the infection. The study assumes that infection with COVID-19 confers temporary immunity upon recovery.

The recruitment of individuals into the susceptible class is through births at the per capita rate Λ. Following an outbreak of the disease, several containment measures are implemented to control the spread. The susceptible humans acquire infection from an infectious individual via a force of infection βI, where β is the transmission coefficient. The saturated incidence rates given by $\beta SI/1 + \eta I$ and $\beta_1 VI/1 + \eta I$ tend to the saturation level when I grows large. The constant η measures the saturation effects caused by infective individuals in the presence of containment measures. The proportion of vaccination is given by γ, $(0 < \gamma \leq 1)$. The transmission coefficient of the vaccinees is denoted by $\beta_1 := (1 - \vartheta)\beta$, where the parameter ϑ, $(0 < \vartheta \leq 1)$ measures the vaccine efficacy. The vaccinees are considered to have acquired partial immunity against COVID-19 subject to the type of vaccine (efficacy level)

administered to an individual. The transmission coefficient of the vaccinees, $\beta_1 < \beta$ since the vaccinees are assumed to have acquired a vaccine-induced immunity [27, 28]. The rate at which exposed individuals become infectious is denoted by ε. The rates of natural and disease-induced mortality are μ and δ, respectively. The recovery rate from the infection is taken as λ.

The above model description translates into the following schematic flow diagram in Figure 1.

From the description above, the corresponding mathematical model is represented by the following set of ordinary differential equations:

$$\begin{aligned}
\frac{dS}{dt} &= \Lambda - \frac{\beta SI}{1+\eta I} - (\mu+\gamma)S,\\
\frac{dV}{dt} &= \gamma S - \frac{\beta_1 VI}{1+\eta I} - \mu V,\\
\frac{dE}{dt} &= \frac{(\beta S + \beta_1 V)I}{1+\eta I} - (\mu+\varepsilon)E,\\
\frac{dI}{dt} &= \varepsilon E - (\mu+\lambda+\delta)I,\\
\frac{dR}{dt} &= \lambda I - \mu R,
\end{aligned} \tag{1}$$

where $\beta_1 < \beta$, $S = S(t), V = V(t), E = E(t)$, $I = I(t)$, $R = R(t)$, $(S, V, E, I, R) \in \mathbb{R}_+^5$.

3. Well-Posedness of the Model

In this section, well-posedness of the model solutions is discussed. Model (1) describes the human population, and therefore, its solutions, as shown below, are positive and bounded for all time $t \geq 0$.

3.1. Boundedness of Solutions. Model (1) is analyzed in a suitable feasible region

$$\Omega = \left\{(S, V, E, I, R)(t) \in \mathbb{R}_+^5 : S(t) + V(t) + E(t) + I(t) + R(t) \leq \frac{\Lambda}{\mu}\right\}, \tag{2}$$

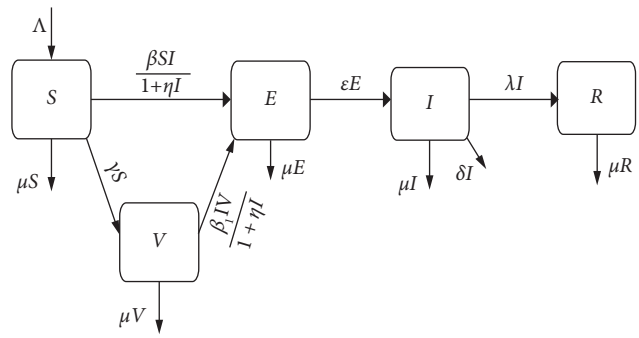

Figure 1: A schematic flow diagram of the COVID-19 dynamics model with vaccination.

where $S(t) + V(t) + E(t) + I(t) + R(t) = N(t)$ gives the total human population.

Using Proposition 1 below, the model solutions are shown to be bounded for all $t \geq 0$ in the region Ω.

Proposition 1. *For all time $t \geq 0$, the solutions of model (1) are invariant in the region Ω.*

Proof. The solutions of model (1) are positively invariant of Ω, i.e., all solutions start in Ω and remain in the region Ω for all $t \geq 0$. The rate of change of human population $N(t)$ is given by

$$\frac{\mathrm{d}N}{\mathrm{d}t} = \frac{\mathrm{d}S}{\mathrm{d}t} + \frac{\mathrm{d}V}{\mathrm{d}t} + \frac{\mathrm{d}E}{\mathrm{d}t} + \frac{\mathrm{d}I}{\mathrm{d}t} + \frac{\mathrm{d}R}{\mathrm{d}t}. \tag{3}$$

which implies that

$$\frac{dN}{dt} \leq \Lambda - \mu N. \tag{4}$$

By variation-of-constant formula, it follows that

$$\limsup_{t \longrightarrow +\infty} N(t) \leq \frac{\Lambda}{\mu}. \tag{5}$$

Thus, $N(t) \leq \Lambda/\mu$. This implies that the solution set $\{S(t), V(t), E(t), I(t), R(t)\}$ is bounded in the feasible region Ω, i.e.,

$$\Omega = \left\{\{(S(t), V(t), E(t), I(t), R(t)\} | S(t) + V(t) + E(t) + I(t) + R(t) \leq \frac{\Lambda}{\mu}, \quad (S, V, E, I, R)(0) \geq 0\right\}. \tag{6}$$

Hence, all solutions of model (1) are bounded in the region Ω. □

3.2. Positivity of Solutions

Proposition 2. *All solution sets $\{S(t), V(t), E(t), I(t), R(t)\}$ of model (1) with non-negative initial conditions are positive $\forall t > 0$.*

Proof. Considering the first equation in model (1), that is,

$$\frac{dS}{dt} = \Lambda - \frac{\beta SI}{1+\eta I} - (\mu+\gamma)S, \tag{7}$$

where

$$\frac{dS}{dt} \geq -\left[\frac{\beta I}{1+\eta I} + (\mu+\gamma)\right]S. \tag{8}$$

integration by variable separation to get

$$\int \frac{dS}{S} \geq \int -\left[\frac{\beta I}{1+\eta I} + (\mu+\gamma)\right]\mathrm{d}t. \tag{9}$$

thus

$$S(t) \geq S(0)\exp -\left\{\int_0^t K d\tau + (\mu+\gamma)t\right\}, \tag{10}$$

where $K = \beta I/1+\eta I$. This implies that

$$S(t) \geq 0 \forall\, t \geq 0. \tag{11}$$

In a similar way, all the other variables can be shown to be positive $\forall t \geq 0$. Hence, all solutions of model (1) are positive in the region Ω.

Clearly, from Propositions 1 and 2, all solutions of model (1) are shown to be positively invariant in the region Ω. Thus, model (1) is mathematically and epidemiologically well posed in a biological feasible region Ω. □

4. The Vaccine Reproduction Number and the Disease-Free Equilibrium

In this section, the disease-free equilibrium and the vaccine reproduction number R_V of the model (1) are computed.

4.1. The Disease-Free Equilibrium. The disease-free equilibrium (DFE) point of model (1) is defined as the state in which there is no COVID-19 infection in the population under study.

Proposition 3. *There exists a DFE of model (1) given by*

$$E_0 = \left(S^0, V^0, E^0, I^0, R^0\right) = \left\{\frac{\Lambda}{\mu+\gamma}, \frac{\gamma\Lambda}{\mu(\mu+\gamma)}, 0, 0, 0\right\}. \tag{12}$$

Proof. At the disease-free equilibrium point, there is no infection in the population. Therefore, with $E = I = R = 0$, then model (1) is given as follows:

$$\begin{aligned}
\Lambda - \frac{\beta SI}{1+\eta I} - (\mu+\gamma)S &= 0,\\
\gamma S - \frac{\beta_1 VI}{1+\eta I} - \mu V &= 0,\\
\frac{(\beta S + \beta_1 V)I}{1+\eta I} - (\mu+\varepsilon)E &= 0,\\
\varepsilon E - (\mu+\lambda+\delta)I &= 0,\\
\lambda I - \mu R &= 0.
\end{aligned} \tag{13}$$

Solving model (13) $S^0 = \Lambda/\mu+\gamma$ and $V^0 = \gamma\Lambda/\mu(\mu+\gamma)$. Therefore, model (1) has a disease-free equilibrium given by

$$E_0 = \left[\frac{\Lambda}{\mu+\gamma}, \frac{\gamma\Lambda}{\mu(\mu+\gamma)}, 0, 0, 0\right]. \tag{14}$$

□

4.2. Reproduction Number. The basic reproduction number, usually denoted by R_0, is defined as the average number of secondary infections due to a single infectious individual introduced into a fully susceptible population during his/her period of infectivity [29]. The basic reproduction number is the spectral radius of the matrix, FV^{-1}, $R_0 = \rho(FV^{-1})$, where F and V are the next-generation matrices [30]. The operator FV^{-1}, the next generation matrix, is formed from matrices of partial derivatives of $\mathscr{F}_i$ (the rate of appearance of new infection in the i^{th} compartment) and $\mathscr{V}_i = \mathscr{V}_i^- - \mathscr{V}_i^+$ (the rate of transfer/transition rate in and out of the disease compartment i) with respect to the infected compartments (E and I) evaluated at DFE. The matrices F and V are given by

$$\begin{aligned}
F &= \left(\frac{\partial \mathscr{F}_i(E_0)}{\partial x_j}\right),\\
V &= \left(\frac{\partial \mathscr{V}_i(E_0)}{\partial x_j}\right),
\end{aligned} \tag{15}$$

where the transition matrices F and V evaluated at E_0 are given by

$$F = \begin{pmatrix} 0 & \dfrac{\Lambda\beta\mu + \beta_1\Lambda\gamma}{\mu(\mu+\gamma)} \\ 0 & 0 \end{pmatrix}, \tag{16}$$

and

$$V = \begin{pmatrix} \mu+\varepsilon & 0 \\ -\varepsilon & \mu+\lambda+\delta \end{pmatrix}. \tag{17}$$

Matrix V is invertible and

$$V^{-1} = \begin{pmatrix} \dfrac{1}{\mu+\varepsilon} & 0 \\ \dfrac{\varepsilon}{(\mu+\varepsilon)(\mu+\lambda+\delta)} & \dfrac{1}{\mu+\lambda+\delta} \end{pmatrix}. \tag{18}$$

Thus, the matrix FV^{-1} is

$$FV^{-1} = \begin{pmatrix} \dfrac{\Lambda\varepsilon\beta(\mu+(1-\vartheta)\gamma)}{\mu(\mu+\gamma)(\mu+\varepsilon)(\mu+\lambda+\delta)} & \dfrac{\Lambda\beta(\mu+(1-\vartheta)\gamma)}{\mu(\mu+\gamma)(\mu+\varepsilon)(\mu+\lambda+\delta)} \\ 0 & 0 \end{pmatrix}. \tag{19}$$

Since model (1) involves vaccination as an intervention, its associated reproduction number is called the vaccine reproduction number denoted by R_V. This is the threshold quantity that can predict the spread of the disease in a given

population in the presence of vaccination. The vaccine reproduction number computed by using the next-generation matrix approach above is given by

$$R_V = \frac{\Lambda\varepsilon\beta(\mu + (1-\vartheta)\gamma)}{\mu(\mu+\varepsilon)(\mu+\lambda+\delta)(\mu+\gamma)},$$
$$R_V = R_0\left[\frac{\mu + (1-\vartheta)\gamma}{\mu+\gamma}\right]. \tag{20}$$

If the vaccine efficacy $\vartheta = 0$, then $R_v = R_0$ which is the basic reproduction number given by $R_0 = \Lambda\varepsilon\beta/\mu(\mu+\varepsilon)(\mu+\lambda+\delta)$.

The vaccine reproduction number, R_V, is the measure of the severity of an epidemic in the presence of vaccination and one of the most important parameters since it determines whether or not the disease will invade a population. Epidemiologically, if $R_V < 1$, then by definition, the infection does not spread in the population. On the other hand, if $R_V > 1$, then the infection spreads in the population and may result into an epidemic.

5. Sensitivity Analysis

The degree to which an input parameter influences a model's output is known as parameter sensitivity. Sensitivity analysis of the basic reproductive number can be used to develop a mitigation strategy that will slow the spread of the pandemic by lowering R_V [14]. Sensitive parameters are those that have a significant impact on the transmission dynamics of an infection. Using the normalized forward sensitivity indices [31], the sensitivity indices are computed by

$$\Upsilon_M^{R_V} = \frac{\partial R_V}{\partial M} \times \frac{M}{R_V}, \tag{21}$$

where M is the parameter whose sensitivity index is computed.

Table 1 gives a summary of the sensitivity indices of R_V evaluated at the baseline parameters values given in Table 2.

From the sensitivity analysis as presented in Table 1, an increase of the rate of vaccination γ by 1% leads to a decrease of the effective reproduction R_V by 0.89844626%. An increase of the vaccine efficacy ϑ by 1% leads to a decrease in the effective reproductive number R_V by 0.9990436%. Clearly, the rate of vaccination and the vaccine efficacy are among the sensitive parameters of R_V. An increase in the rate of vaccination, with high vaccine efficacy, leads to a decrease in the vaccine reproduction number. Consequently, control strategies should target an increased rate of vaccination and administration of vaccines of high efficacy levels.

Table 1: Sensitivity indices of R_V with respect to the model parameters.

Parameter	Description	Sensitivity index
Λ	Recruitment rate	+1
β	Transmission coefficient	+1
ε	Transition rate from E to I	−0.999843
μ	Natural death rate	$+7.81816576\times10^{-5}$
γ	Rate of vaccination	−0.8984463
ϑ	Vaccine efficacy	−0.9998436
λ	Recovery rate	−0.999679
δ	Disease mortality rate	−0.000008237

Table 2: The descriptive summary of the model parameters.

Parameter	Description	Unit/value units	Source
Λ	Recruitment rate	3.178×10^{-5} day^{-1}	[28]
μ	Natural death rate	3.91×10^{-5} day^{-1}	[10]
δ	Disease mortality rate	0.103×10^{-5} day^{-1}	[28]
β	Transmission coefficient	0.02 day^{-1}	Estimated
β_1	Transition rate from V to E	0.05 day^{-1}	Estimated
ϑ	Vaccine efficacy	(0–1.0)	Variable
γ	Rate of vaccination	(0–1.0)	Variable
ε	Transition rate from E to I	0.5 day^{-1}	Estimated
η	Human saturation constant	0.05	Estimated
λ	Human recovery rate	0.125 day^{-1}	[32]

6. Optimal Analysis with Vaccination Program as a Control Intervention

An optimal control problem is constructed to control the spread of the COVID-19 virus and optimize the vaccination program. Therefore, in this section, optimal control is performed to understand the effects of the sensitive parameters on the optimum vaccination program. To determine the optimum vaccination program for COVID-19, let the variables γ^* and $\beta_1^* =: (1-\vartheta)\beta$ be the control variables. As a result, an optimal control problem is constructed, with the goal of reducing the number of individuals infected with COVID-19. The following objective function is created to accomplish this:

$$J = \int_0^\tau \left[P_0 S + P_1 V + P_2 E + P_3\gamma^2 + P_4\beta_1^2\right]\mathrm{d}t. \tag{22}$$

where $[0,\tau]$ is the entire time horizon over the control applied and P_0, P_1, P_2, P_3, P_4 are positive weights that balance the relative importance of terms in the objective functional J. An optimal control γ^*, β_1^* is chosen as

$$J(\gamma^*, \beta_1^*) = \min\{J(\gamma, \beta_1)\}. \tag{23}$$

such that (γ, β_1) are measurable with $0 \le \gamma \le \beta_1 \le 1$. This is the necessary condition that the optimal control must

satisfy from Pontryagin's maximum principle [33, 34]. The Hamiltonian function is

$$H = P_0 S + P_1 V + P_2 E + P_3 \gamma^2 + P_4 \beta_1^2 + \Phi_s \left[\Lambda - \frac{\beta S I}{1+\eta I} - (\mu+\gamma) S \right] + \Phi_V \left[\gamma S - \frac{\beta_1 V I}{1+\eta I} - \mu V \right] + \Phi_E \left[\frac{(\beta S + \beta_1 V) I}{1+\eta I} - (\mu+\varepsilon) E \right] + \Phi_I [\varepsilon E - (\mu+\lambda+\delta) I] + \Phi_R [\lambda I - \mu R], \tag{24}$$

where Φ_S, Φ_V, Φ_E, Φ_I, and Φ_R are the adjoint variables. To obtain the expression of optimal controls in order to minimize the number of infections in the population and the cost of control strategies, the following proposition is applied.

Proposition 4. *For the optimal control (γ, β_1) that minimizes $J(\gamma, \beta_1)$, the adjoint variables Φ_S, Φ_V, Φ_E, Φ_I, and Φ_R satisfy the following ordinary differential equations:*

$$\begin{aligned}
\frac{d\Phi_S}{dt} &= P_0 - \Phi_S \frac{\beta I}{1+\eta I} - (\mu+\gamma)\Phi_S + \gamma \Phi_V + \Phi_E \frac{\beta I}{1+\eta I}, \\
\frac{d\Phi_V}{dt} &= P_1 - \Phi_V \frac{\beta I}{1+\eta I} - \mu \Phi_V + \Phi_E \frac{\beta_1 I}{1+\eta I}, \\
\frac{d\Phi_E}{dt} &= P_2 - (\mu+\varepsilon)\Phi_E + \varepsilon \Phi_I, \\
\frac{d\Phi_I}{dt} &= -\Phi_S \frac{\beta S}{(1+\eta I)^2} - \Phi_V \frac{\beta_1 V}{(1+\eta I)^2} + \Phi_E \frac{(\beta S + \beta_1 V)}{(1+\eta I)^2} \\
&\quad - \Phi_I (\mu+\lambda+\delta) + \lambda \Phi_R, \\
\frac{d\Phi_R}{dt} &= \mu \Phi_R.
\end{aligned} \tag{25}$$

with transversality conditions

$$\Phi_S(\tau) = \Phi_V(\tau) = \Phi_E(\tau) = \Phi_I(\tau) = \Phi_R(\tau) = 0. \tag{26}$$

Thus, the optimal control takes the characterization form, which is given as follows:

$$\gamma^* = \max\left[0, \min\left(1, \frac{S(\Phi_S - \Phi_V)}{2P_3}\right)\right], \tag{27}$$

$$\beta_1^* = \max\left[0, \min\left(1, \frac{VI(\Phi_V - \Phi_E)}{2(1+\eta I)P_4}\right)\right]. \tag{28}$$

Proof. The Hamiltonian H in equation (25) is differentiated with respect to the state variables, S, V, E, I, R, respectively. Thus, the adjoint of the system can be written as

$$\Phi_M = -\frac{\partial H}{\partial M}, \tag{29}$$

for

$$M = \{S, V, E, I, R\}. \tag{30}$$

By Pontryagin's maximum principle [34], H can be maximized with respect to γ and β_1, that is,

$$\begin{aligned}
0 &= \frac{\partial H}{\partial \gamma}\Big|_{\gamma^*} = 2P_3\gamma - \Phi_S S - \Phi_V S, \\
\Rightarrow \gamma^* &= \frac{S(\Phi_S - \Phi_V)}{2P_3}. \\
0 &= \frac{\partial H}{\partial \beta_1}\Big|_{\beta_1^*} = 2P_4\beta_1 - \Phi_V \frac{VI}{1+\eta I} + \Phi_E \frac{VI}{1+\eta I}, \\
\Rightarrow \beta_1^* &= \frac{VI(\Phi_V - \Phi_E)}{2(1+\eta I)P_4}.
\end{aligned} \tag{31}$$

Taking the bounds on γ and β_1 into account, the characterization of γ^* and β_1^* is obtained as shown in (27) and (28), respectively. Now, using the control arguments $0 \le \gamma \le \beta_1 \le 1$, then we obtain

$$\begin{aligned}
\gamma^* &= \begin{cases} 0 & \text{if } \xi_1^* \le 0 \\ \xi_1^* & \text{if } 0 < \xi_1^* < 1 \\ 1 & \text{if } \xi_1^* \ge 1 \end{cases}, \\
\beta_1^* &= \begin{cases} 0 & \text{if } \xi_2^* \le 0 \\ \xi_2^* & \text{if } 0 < \xi_2^* < 1 \\ 1 & \text{if } \xi_2^* \ge 1 \end{cases},
\end{aligned} \tag{32}$$

where

$$\begin{aligned}
\xi_1^* &= \frac{S(\Phi_S - \Phi_V)}{2P_3}, \\
\xi_2^* &= \frac{VI(\Phi_V - \Phi_E)}{2(1+\eta I)P_4}.
\end{aligned} \tag{33}$$

Since the optimal control switches at most once, then the control objective function constructed in this study is at optimum.

In recent decades, control theory has been widely applied in many fields. Optimal control, particularly in epidemiology, could be very useful in controlling mathematical models depicting the spread of infectious diseases [35]. The appropriate regulation of disease dynamics is specified in the form of restrictions according to the biological

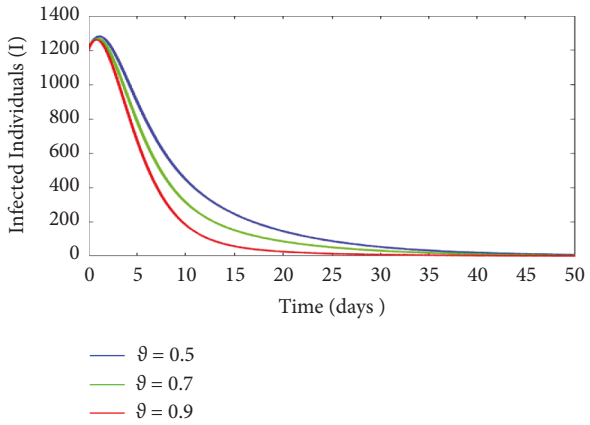

Figure 2: The effect of variation in vaccine efficacy (ϑ) on infection dynamics.

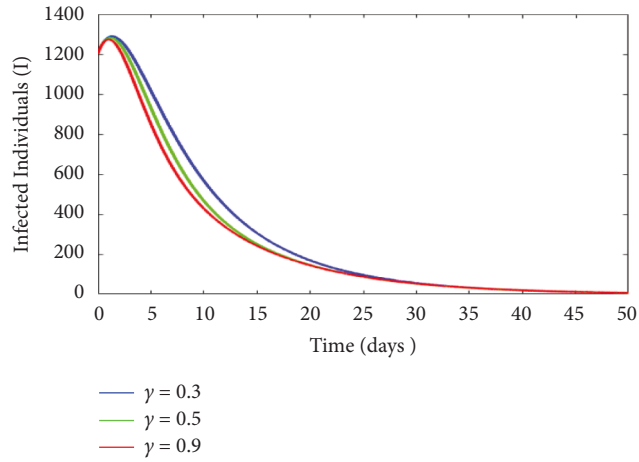

Figure 3: The effect of variation in the vaccination rate (γ) on infection dynamics.

interpretation of the objective function. The control's objectives must be met exclusively within these limits. Furthermore, lowering illness prevalence requires reducing the total number of infectious cases. This entails increasing the rate of vaccination (γ) while decreasing the coefficient of contracting the infection $\beta_1 = (1 - \vartheta)\beta$. Increased vaccination rates and the administering of highly efficacious vaccines would help maximize control strategies against COVID-19 transmission dynamics. □

7. Numerical Simulation and Discussion

The parameters used for simulation are obtained from literature, and others are estimates, as listed in Table 2. These parameter values are varied within realistic limits.

For purposes of simulation, unless otherwise stated, the initial populations are taken to be $S(0) = 3000$, $V(0) = 2000$, $E(0) = 1500$, $I(0) = 1200$, and $R(0) = 1000$.

The numerical simulation aims to analyze the change in the state of COVID-19 virus progression over time, as well as the impact of variation in the vaccination rate and vaccine efficacy on COVID-19 transmission dynamics. This is accomplished by varying the parameters ϑ and γ while holding the other parameters constant. Simulation analyses of the model (1) are presented in Figures 2 and 3.

Figure 2 shows the effect of variation in vaccine efficacy (ϑ) on infection dynamics. When the vaccine administered is of high efficacy, say 90% efficacy, it would take less time for the pool of infected individuals to reduce. On the other hand, when the vaccine efficacy is low, it would take a longer time for the number of infected individuals to reduce, and therefore, COVID-19 infection would persist in the population. Figure 3 shows the effect of variation in the vaccination rate (γ) on infection dynamics. It is shown that when the rate of vaccination is high, the number of infected individuals decreases sharply and vice versa. Figure 4 shows the graph of the vaccine reproduction number R_V against the vaccination rate (γ). It is observed that with an increase in the rate of vaccination (γ), the vaccine reproduction number decreases sharply. Figure 5 shows the 3D plot of the vaccine reproduction number R_V against the rate of vaccination (γ)

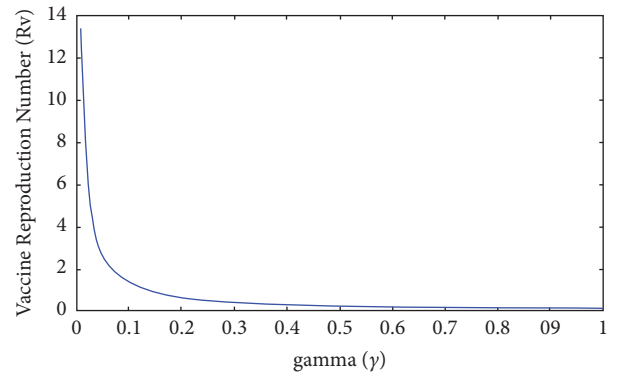

Figure 4: Plot of the vaccine reproduction number R_V against the rate of vaccination (γ).

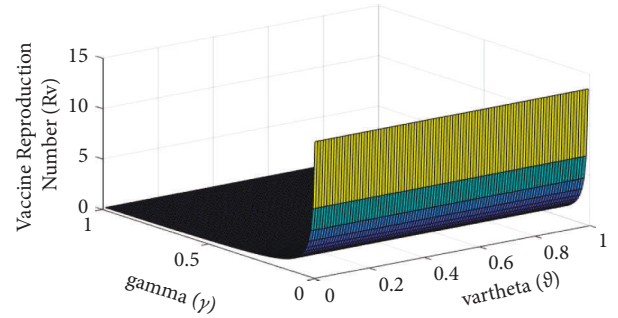

Figure 5: Plot of the vaccine reproduction number R_V against the rate of vaccination (γ) and vaccine efficacy (ϑ).

and vaccine efficacy (ϑ). It is observed that with an increase in both the rate of vaccination and vaccine efficacy, the vaccine reproduction number decreases sharply.

Vaccination offers a very powerful method of COVID-19 disease control. The critical level of vaccination of above 50% with an > 80% vaccine efficacy level would be required to reduce the severity and eventually eradicate the infection from the population. Herd immunity against COVID-19 can be achieved by immunizing a significant proportion of the

susceptible population. To prevent a large outbreak in the future, in addition to vaccination, a variety of other control measures (e.g., COVID-19 protocols such as the use of masks, social distancing, proper hygiene, and so on) are required [14, 36].

8. Conclusion

In this paper, the effect of vaccination as an intervention is investigated through an SVEIR model. The well-posedness of the model and the existence of disease-free equilibrium are shown. Sensitivity analysis here suggests that the rate of vaccination, γ, and the vaccine efficacy ϑ are among the most influential parameters of R_V. For optimal control, increasing the vaccination rate and administering highly efficacious vaccines would help maximize control strategies against COVID-19 transmission dynamics. This is illustrated by the numerical simulations. This study, like others [19, 37, 38], confirms that vaccination may possibly eradicate the infection in the population. Future research could focus on an age-dependent SVEIR model to determine the suitable vaccination strategy to be applied with respect to age.

Data Availability

The data used to support the study's findings are included within the article.

Conflicts of Interest

The authors declare that they have no conflicts of interest.

Acknowledgments

The work was supported by the Masinde Muliro University of Science and Technology, Postgraduate Merit Scholarship Award.

References

[1] V. V. Albani, J. Loria, E. Massad, and J. P. Zubelli, "The impact of COVID-19 vaccination delay: a modelling study for chicago and NYC data," 2021, https://arxiv.org/abs/2102.12299.

[2] S. Orangi, J. Pinchoff, D. Mwanga et al., "Assessing the level and determinants of COVID-19 vaccine confidence in Kenya," *Vaccines*, vol. 9, no. 8, pp. 936–947, 2021.

[3] S. P. Adhikari, S. Meng, Y. J. Wu et al., "Epidemiology, causes, clinical manifestation and diagnosis, prevention and control of coronavirus disease (COVID-19) during the early outbreak period: a scoping review," *Infectious diseases of poverty*, vol. 9, no. 1, pp. 29–12, 2020.

[4] A. Aleta, D. Martin-Corral, A. Pastore y Piontti et al., "Modelling the impact of testing, contact tracing and household quarantine on second waves of COVID-19," *Nature Human Behaviour*, vol. 4, no. 9, pp. 964–971, 2020.

[5] R. P. Mondaini, *Trends in Biomathematics: Modeling Cells, Flows, Epidemics, and the Environment*, Springer International Publishing, Berlin, Germany, 2020.

[6] R. Rappuoli, C. W. Mandl, S. Black, and E. De Gregorio, "Vaccines for the twenty-first century society," *Nature Reviews Immunology*, vol. 11, no. 12, pp. 865–872, 2011.

[7] M. D. Samsuzzoha, *A Study on Numerical Solutions of Epidemic Models (Doctoral Dissertation, PhD Thesis*, Swinburne University of Technology, Australia, 2012.

[8] N. Steyn, M. J. Plank, R. N. Binny, S. C. Hendy, A. Lustig, and K. Ridings, "A COVID-19 vaccination model for Aotearoa New Zealand," *Scientific Reports*, vol. 12, no. 1, pp. 2720–2811, 2022.

[9] S. Moore, E. M. Hill, L. Dyson, M. J. Tildesley, and M. J. Keeling, "Modelling optimal vaccination strategy for SARS-CoV-2 in the UK," *PLoS Computational Biology*, vol. 17, no. 5, Article ID e1008849, 2021.

[10] M. Amaku, D. T. Covas, F. A. B. Coutinho, R. S. Azevedo, and E. Massad, "Modelling the impact of delaying vaccination against SARS-CoV-2 assuming unlimited vaccine supply," *Theoretical Biology and Medical Modelling*, vol. 18, no. 1, pp. 14–11, 2021.

[11] M. Fudolig and R. Howard, "The local stability of a modified multi-strain SIR model for emerging viral strains," *PLoS One*, vol. 15, no. 12, Article ID e0243408, 2020.

[12] I. Area, F. Ndairou, J. J Nieto, C. J Silva, and D. F M Torres, "Ebola model and optimal control with vaccination constraints," *Journal of Industrial and Management Optimization*, vol. 14, no. 2, pp. 427–446, 2018.

[13] I. A. Baba, B. Kaymakamzade, and E. Hincal, "Two-strain epidemic model with two vaccinations," *Chaos, Solitons & Fractals*, vol. 106, no. 1, pp. 342–348, 2018.

[14] C. T. Deressa, Y. O. Mussa, and G. F. Duressa, "Optimal control and sensitivity analysis for transmission dynamics of Coronavirus," *Results in Physics*, vol. 19, Article ID 103642, 2020.

[15] I. A. Baba and E. Hincal, "A model for Influenza with vaccination and awareness," *Chaos, Solitons & Fractals*, vol. 106, no. 1, pp. 49–55, 2018.

[16] T. A. Perkins and G. Espana, "Optimal control of the COVID-19 pandemic with non-pharmaceutical interventions," *Bulletin of Mathematical Biology*, vol. 82, no. 9, pp. 118–124, 2020.

[17] E. O. Alzahrani, W. Ahmad, M. Altaf Khan, and S. J. Malebary, "Optimal control strategies of Zika virus model with mutant," *Communications in Nonlinear Science and Numerical Simulation*, vol. 93, Article ID 105532, 2021.

[18] I. Abdullahi, B. A. Baba, and B. Nasidi, "Optimal Control Model for the Transmission of Novel COVID-19," *Computers, Materials & Continua*, vol. 66, pp. 3089–3106, 2021.

[19] C. E. Wagner, C. M. Saad-Roy, and B. T. Grenfell, "Modelling vaccination strategies for COVID-19," *Nature Reviews Immunology*, vol. 22, no. 3, pp. 139–141, 2022.

[20] Z. H. Shen, Y. M. Chu, M. A. Khan, S. Muhammad, O. A. Al-Hartomy, and M. Higazy, "Mathematical modeling and optimal control of the COVID-19 dynamics," *Results in Physics*, vol. 31, Article ID 105028, 2021.

[21] H. Habenom, M. Aychluh, D. L. Suthar, Q. Al-Mdallal, and S. D. Purohit, "Modeling and analysis on the transmission of covid-19 Pandemic in Ethiopia," *Alexandria Engineering Journal*, vol. 61, no. 7, pp. 5323–5342, 2022.

[22] M. Zamir, T. Abdeljawad, F. Nadeem, A. Wahid, and A. Yousef, "An optimal control analysis of a COVID-19 model," *Alexandria Engineering Journal*, vol. 60, no. 3, pp. 2875–2884, 2021.

[23] A. M. Mishra, S. D. Purohit, K. M. Owolabi, and Y. D. Sharma, "A nonlinear epidemiological model considering asymptotic and quarantine classes for SARS CoV-2 virus," Chaos," *Solitons & Fractals*, vol. 138, Article ID 109953, 2020.

[24] M. S. Alqarni, M. Alghamdi, T. Muhammad, A. S. Alshomrani, and M. A. Khan, "Mathematical modeling

for novel coronavirus (COVID-19) and control," *Numerical Methods for Partial Differential Equations*, vol. 38, no. 4, pp. 760–776, 2022.

[25] S. A. Lauer, K. H. Grantz, Q. Bi et al., "The incubation period of coronavirus disease 2019 (COVID-19) from publicly reported confirmed cases: estimation and application," *Annals of Internal Medicine*, vol. 172, no. 9, pp. 577–582, 2020.

[26] M. Cevik, K. Kuppalli, J. Kindrachuk, and M. Peiris, "Virology, transmission, and pathogenesis of SARS-CoV-2," *bmj*, vol. 371, 2020.

[27] S. H. Hodgson, K. Mansatta, G. Mallett, V. Harris, K. R. W. Emary, and A. J. Pollard, "What defines an efficacious COVID-19 vaccine? A review of the challenges assessing the clinical efficacy of vaccines against SARS-CoV-2," *The Lancet Infectious Diseases*, vol. 21, no. 2, pp. 26–35, 2021.

[28] D. Martínez-Rodríguez, G. Gonzalez-Parra, and R. J. Villanueva, "Analysis of key factors of a SARS-CoV-2 vaccination program: a mathematical modeling approach," *Epidemiologia*, vol. 2, no. 2, pp. 140–161, 2021.

[29] R. M. Anderson and R. M. May, *Infectious Disease of Human: Dynamics and Control*, Oxford University Press, London, UK, 1991.

[30] P. Van-den Driessche and J. Watmough, "Reproduction numbers and sub-threshold endemic equilibria for compartmental models of disease transmission," *Mathematical Biosciences*, vol. 180, no. 2, pp. 29–48, 2002.

[31] N. Chitnis, J. M. Hyman, and J. M. Cushing, "Determining important parameters in the spread of malaria through the sensitivity analysis of a mathematical model," *Bulletin of Mathematical Biology*, vol. 70, no. 5, pp. 1272–1296, 2008.

[32] E. Eryarsoy, D. Delen, B. Davazdahemami, and K. Topuz, "A novel diffusion-based model for estimating cases, and fatalities in epidemics: the case of COVID-19," *Journal of Business Research*, vol. 124, pp. 163–178, 2021.

[33] L. S. Pontryagin, V. G. Boltyanskii, R. V. Gamkrelidze, E. F. Mishchenko, K. N. Trirogoff, and L. W. Neustadt, *LS Pontryagin Selected Works: The Mathematical Theory of Optimal Processes*, Routledge, London, UK, 2018.

[34] L. S. Pontryagin, *Mathematical Theory of Optimal Processes*, CRC Press, Boca Raton, Florida, 1987.

[35] S. İğret Araz, "Analysis of a Covid-19 model: optimal control, stability and simulations," *Alexandria Engineering Journal*, vol. 60, no. 1, pp. 647–658, 2021.

[36] M. Kimathi, S. Mwalili, V. Ojiambo, and D. K. Gathungu, "Age-structured model for COVID-19: effectiveness of social distancing and contact reduction in Kenya," *Infectious Disease Modelling*, vol. 6, pp. 15–23, 2021.

[37] J. Demongeot, Q. Griette, P. Magal, and G. Webb, "Modeling vaccine efficacy for COVID-19 outbreak in New York city," *Biology*, vol. 11, no. 3, p. 345, 2022.

[38] K. Liu and Y. Lou, "Optimizing COVID-19 vaccination programs during vaccine shortages: a review of mathematical models," *Infectious Disease Modelling*, vol. 7, 2022.